



Since January 2020 Elsevier has created a COVID-19 resource centre with free information in English and Mandarin on the novel coronavirus COVID-19. The COVID-19 resource centre is hosted on Elsevier Connect, the company's public news and information website.

Elsevier hereby grants permission to make all its COVID-19-related research that is available on the COVID-19 resource centre - including this research content - immediately available in PubMed Central and other publicly funded repositories, such as the WHO COVID database with rights for unrestricted research re-use and analyses in any form or by any means with acknowledgement of the original source. These permissions are granted for free by Elsevier for as long as the COVID-19 resource centre remains active.

Angiotensin II induces reactive oxygen species, DNA damage, and T-cell apoptosis in severe COVID-19



Lucy Kundura, PhD,^a Sandrine Gimenez, BSc,^a Renaud Cezar, MSc,^b Sonia André, PhD,^c Mehwish Younas, PhD,^a Yea-Lih Lin, PhD,^a Pierre Portalès, PharmD,^d Claire Lozano, PharmD, PhD,^d Charlotte Boule, MD,^e Jacques Reynes, MD, PhD,^e Thierry Vincent, MD, PhD,^d Clément Mettling, PhD,^a Philippe Pasero, PhD,^a Laurent Muller, MD, PhD,^f Jean-Yves Lefrant, MD, PhD,^f Claire Roger, MD, PhD,^f Pierre-Géraud Claret, MD, PhD,^g Sandra Duvnjak, MD,^h Paul Loubet, MD, PhD,ⁱ Albert Sotto, MD, PhD,ⁱ Tu-Anh Tran, MD, PhD,^j Jérôme Estaquier, PhD,^{c,k*} and Pierre Corbeau, MD, PhD^{a,b*}
 Montpellier, Nîmes, and Paris, France; and Québec City, Québec, Canada

Background: Lymphopenia is predictive of survival in patients with coronavirus disease 2019 (COVID-19).

Objective: The aim of this study was to understand the cause of the lymphocyte count drop in severe forms of severe acute respiratory syndrome coronavirus 2 (SARS-CoV-2) infection.

Methods: Monocytic production of reactive oxygen species (ROS) and T-cell apoptosis were measured by flow cytometry, DNA damage in PBMCs was measured by immunofluorescence, and angiotensin II (AngII) was measured by ELISA in patients infected with SARS-CoV-2 at admission to an intensive care unit (ICU) (n = 29) or not admitted to an ICU (n = 29) and in age- and sex-matched healthy controls.

Results: We showed that the monocytes of certain patients with COVID-19 spontaneously released ROSs able to induce DNA damage and apoptosis in neighboring cells. Of note, high ROS production was predictive of death in ICU patients.

Accordingly, in most patients, we observed the presence of DNA damage in up to 50% of their PBMCs and T-cell apoptosis.

Moreover, the intensity of this DNA damage was linked to lymphopenia. SARS-CoV-2 is known to induce the

internalization of its receptor, angiotensin-converting enzyme 2, which is a protease capable of catabolizing AngII. Accordingly, in certain patients with COVID-19 we observed high plasma levels of AngII. When looking for the stimulus responsible for their monocytic ROS production, we revealed that AngII triggers ROS production by monocytes via angiotensin receptor I. ROSs released by AngII-activated monocytes induced DNA damage and apoptosis in neighboring lymphocytes.

Conclusion: We conclude that T-cell apoptosis provoked via DNA damage due to the release of monocytic ROSs could play a major role in COVID-19 pathogenesis. (*J Allergy Clin Immunol* 2022;150:594-603.)

Key words: SARS-CoV-2, ACE2, oxidative stress, antioxidant, angiotensin II receptor, DNA oxidation, programmed cell death, lymphopenia

Coronavirus 2019 disease (COVID-19) is an infectious disease caused by severe acute respiratory syndrome coronavirus 2 (SARS-CoV-2). The most severe forms of COVID-19 are due to acute lung damage, which is strongly linked to hyperactivation of the immune system.¹ A hallmark of critical COVID-19 is lymphopenia,² which is observed in up to 63% of patients with COVID-19 and predictive of an unfavorable outcome.³ Yet, the cause of peripheral blood T-cell, B-cell, and natural killer (NK) cell loss remains unclear. Indeed, this loss may be the consequence of a decrease in lymphocyte production, the trapping of these cells in the respiratory tract, and/or a high rate of lymphocyte death. As lymphocyte counts are strongly predictive of survival, understanding the causes of lymphopenia is of major importance.

Various RNA viruses have been reported to induce ROS production and antioxidant system depletion. For instance, the influenza virus increases the level of ROS production in the host cells and decreases the concentration of antioxidants.⁴ Moreover, the oxidative stress provoked by the virus is responsible for lung damage that may be prevented by antioxidants or by targeting nicotinamide adenine dinucleotide phosphate (NADPH) oxidase-2.⁴ Likewise, respiratory syncytial virus infection causes ROS expression⁵ and decreases the expression of antioxidant genes, contributing to bronchiolitis.⁶ SARS-CoV-1 modifies the

From ^athe Institute of Human Genetics, UMR9002, CNRS, Montpellier University, Montpellier; ^bthe Immunology Department, ^cthe Surgical Intensive Care Department, ^ethe Medical and Surgical Emergency Department, ^hthe Gerontology Department, ⁱthe Infectious Diseases Department, and ^jthe Pediatrics Department, Nîmes University Hospital; ^cthe INSERM U1124, Université Paris Descartes; ^dthe Immunology Department and ^ethe Infectious Diseases Department, Montpellier University Hospital; and ^hthe Laval University Research Center; Québec City.

*These authors contributed equally to this work.

Supported by the University Hospital of Nîmes (grant NIMAO/2020/COVID/PC-01 [to P.C.]), the Fondation pour la Recherche Médicale, and the Agence Nationale de Recherche (grant 216261 [to J.E.]).

Disclosure of potential conflict of interest: P. Corbeau received a grant from AbbVie. The rest of the authors declare that they have no relevant conflicts of interest.

Received for publication January 11, 2022; revised April 24, 2022; accepted for publication June 17, 2022.

Available online July 14, 2022.

Corresponding author: Pierre Corbeau, MD, PhD, Institute of Human Genetics, 141 rue de la Cardonille, 34396 Montpellier cedex 5, France. E-mail: pcorbeau@igh.cnrs.fr.

The CrossMark symbol notifies online readers when updates have been made to the article such as errata or minor corrections

0091-6749/\$36.00

© 2022 American Academy of Allergy, Asthma & Immunology

<https://doi.org/10.1016/j.jaci.2022.06.020>

Abbreviations used

ACE2:	Angiotensin-converting enzyme 2
AngII:	Angiotensin II
AT1:	Angiotensin receptor type 1
AU:	Arbitrary unit
COVID-19:	Coronavirus disease 2019
DCFH-DA:	Dichlorodihydrofluorescein diacetate
DPI:	Diphenyleiiodonium
HD:	Healthy donor
ICU:	Intensive care unit
IQR:	Interquartile range
NAC:	N-acetylcysteine
NADP:	Nicotinamide adenine dinucleotide phosphate
NK:	Natural killer
ROS:	Reactive oxygen species
SARS-CoV-2:	Severe acute respiratory syndrome coronavirus 2

oxidoreductase system of the mitochondria via interaction between its nonstructural protein 10 and cytochrome oxidase II.⁷ In line with this mechanism, oxidative stress has been reported in the lungs of SARS-CoV-1-infected mice.⁸ Likewise, SARS-CoV-2-infected monocytes overproduce mitochondrial ROSs, and increased expression of oxidative stress-associated genes has been observed in monocytes of bronchoalveolar fluid from patients with COVID-19.⁹ In the peripheral blood of these patients, markers of NADPH oxidase-2 activation,¹⁰ impaired antioxidant activity,¹¹ and oxidative stress¹² have been revealed as possibly being linked to the severity of the disease.

As ROSs can cause DNA damage resulting in apoptosis,¹³ we analyzed the level of monocytic ROS production in patients with COVID-19 at different stages, as well as its causes and consequences.

METHODS

Study design

This was an observational, monocentric, case-control study. Adults with positive nasopharyngeal swabs for SARS-CoV-2 RNA by RT-PCR were consecutively recruited at the Nîmes University Hospital. Patients were either recruited on the day of their admission to an intensive care unit (ICU) or at admission to the Tropical and Infectious Diseases Department (the non-ICU group). No outlier was excluded. All of the replicates were biologic. This study was approved by the French Ethics Committee, Île-de-France 1. All patients provided written informed consent, and the trial was registered (Eudract/IDRCB identifier 2020-A00875-34 and ClinicalTrials identifier NCT04351711).

Cell sorting and coculture

Monocytes were sorted from PBMCs by using CD14-coated microbeads (Miltenyi Biotec, Paris, France). Cells, preincubated or not with diphenyleiiodonium (DPI) or N-acetylcysteine (NAC) for 3 hours at 37°C were washed twice and cocultured in 1- μ m-pore size inserts with BJ cells (fibroblasts established from skin [ATCC CRL-2522]) placed on coverslips in 24-well companion plates. PBMCs or monocytes and BJ cells were cocultured in a 2:1 ratio in 1:1 Dulbecco modified Eagle medium and RPMI culture medium supplemented with 10% heat-inactivated FBS for 3 days. Camptothecin (10 μ M) was used on the BJ cells for 45 minutes at 37°C. LPS (1 μ g/mL) or angiotensin II (AngII) (75 pM) was added to the cells in a 500- μ L final volume of RPMI culture medium without serum and incubated at 37°C for 30 minutes. The cells were washed and fixed for further staining.

Immunofluorescence

PBMC adherence on coverslips was obtained by using 20 μ g/mL of polylysine in serum-free RPMI culture medium for 2 hours at room temperature. Coverslips with cocultured BJ cells were washed twice, fixed with 2% paraformaldehyde in PBS for 10 minutes, rinsed again with PBS, and permeabilized with PBS containing 0.1% Triton-X-100 for 10 minutes at room temperature. Thereafter, the coverslips were washed and blocked with PBS containing 10% FBS for 30 minutes. The cells were then incubated with anti- γ -H2AX (Millipore, Guyancourt, France; 1/500) for 1 hour or anti-53BP1 mAb (Millipore; 1/300) in PBS with 10% FBS. The coverslips were rinsed 3 times with PBS and incubated with AF 546 anti-mouse IgG1 (Invitrogen, Villebon sur Yvette, France; 1/2000) secondary antibody for 45 minutes in PBS with 10% FBS at room temperature. After being washed with PBS, DNA was counter stained with 4',6-diamino-2-phenylindole (Sigma-Aldrich, Saint-Quentin-Fallavier, France) for 5 minutes, and coverslips were mounted in fluorescence mounting medium (Prolong Gold, Invitrogen). The slides were kept overnight at 20°C in a dark room. Images were obtained with a Zeiss ApoTome fluorescence microscope (\times 63 magnification and 1.4 numeric aperture for BJ cells and \times 100 magnification and 1.46 numeric aperture for PBMCs) with supporting software and analyzed on Image J and FIJI software systems. The results were expressed as the proportions of BJ cells in microscope fields presenting at least 5 foci per nucleus quantified under microscopy. Cells exposed to camptothecin were used as positive controls.

Flow cytometry

The mAbs used for cell surface staining were CD3-APCA750, CD14-PE, CD16-APC, CD4-APC (all from Beckman Coulter, Villepinte, France) and CD3-BV421 and CD3-AF700 (both from Biolegend, Paris, France). Annexin V-PE (Biolegend) was used according to the manufacturer's guidelines, and the labeling was analyzed at day 6. For ROS quantification, 10⁶ PBMCs were resuspended in 1 μ M dichlorodihydrofluorescein diacetate (DCFH-DA) for 25 minutes at room temperature. Data were acquired on a Navios flow cytometer (Beckman Coulter) from 20,000 gated events per sample and on a MACSQuant analyzer 10 (Miltenyi Biotec) and analyzed using Kaluza software.

ELISA

AngII concentrations were determined by using the Ang II ELISA kit (Enzo Life Sciences, Villeurbanne, France).

Statistical analyses

No data preprocessing was performed. Statistical analyses and graphical presentations were computed with GraphPad Prism, version 6. The D'Agostino and Pearson normality test was performed. Differences between 2 groups were analyzed by using a 2-sided unpaired Student *t* test or Mann-Whitney test as appropriate. Differences between more than 2 groups were analyzed by using 1-way ANOVA, Welch ANOVA, or the Kruskal-Wallis test, as appropriate. We used a 2-sided Spearman rank test to evaluate correlations. A *P* value of < .05 was considered statistically significant.

RESULTS

Patient enrollment

We enrolled 29 patients who were PCR-positive for SARS-CoV-2 infection at admission to an ICU because of an oxygen saturation less than 90% and/or Pao₂ less than 60 mm Hg in room air or an oxygen saturation of less than 95% while receiving 5 liters of oxygen per minute. We also recruited 29 PCR-positive SARS-CoV-2-infected patients at admission to the infectious diseases department (the non-ICU group) because of an oxygen

TABLE I. Bioclinical characteristics of the patients enrolled

Characteristic	Non-ICU patients (n = 29)	ICU patients (n = 29)	Non-ICU vs ICU P value
Age (y), mean (SD)	66.1 (20.9)	69.3 (13.5)	
Age range (y)	29.0-96.0	43.0-95.0	.702
Female sex, no. (%)	16 (55)	13(45)	.600
Male sex, no. (%)	13 (45)	16 (55)	
Any comorbidity, no. (%)	12 (41)	12 (41)	.594
Diabetes, no. (%)	7 (24)	7 (24)	.762
Cancer, no. (%)	4 (14)	2 (7)	.783
Autoimmune disease, no. (%)	1 (3)	0 (0)	.999
Chronic kidney failure, no. (%)	0 (0)	2 (7)	.202
Duration of symptomatology (d), mean (SD)	6.8 (9.4)	11.8 (7.2)	<.001
C-reactive protein level (mg/L), mean (SD)	56.8 (68.1)	115.0 (81.3)	.003
Lactate dehydrogenase level (IU/L), mean (SD)	214.8 (49.9)	416.4 (177.3)	<.001
Absolute lymphocyte count ($\times 10^9/L$), mean (SD)	1.30 (0.53)	0.88 (0.59)	.004
Absolute monocyte count ($\times 10^9/L$), mean (SD)	0.70 (0.36)	0.46 (0.27)	.010

Normal range for C-reactive protein level is 0.9-1.8 mg/L, normal range for lactate dehydrogenase level is 135-214 IU/L, normal range for absolute lymphocyte count is $1.3-3.3 \times 10^9/L$, and normal range for absolute monocyte count is $0.3-0.9 \times 10^9/L$.

saturation less than 96% in room air and/or deterioration in their general condition. Age- and sex-matched HDs (age range 28-95 years) were used as negative controls. The bioclinical characteristics of these patients are shown in [Table I](#).

Monocytes from patients with COVID-19 overproduce ROSs

To test whether monocytes from patients with COVID-19 produced ROSs, we labeled the PBMCs of SARS-CoV-2-infected individuals with DCFH-DA, which reacts with ROSs to give a fluorescent product. [Fig 1, A](#) shows that monocytes from HDs become fluorescent when they are incubated with DCFH-DA and exposed to LPS used as a positive control. This ROS production was prevented by preincubation with the NADPH oxidase inhibitor DPI ([Fig 1, A](#)). In contrast, the spontaneous fluorescence of monocytes from HDs incubated with DCFH-DA was not reduced in the presence of DPI ([Fig 1, A](#)). Monocytes from certain patients with COVID-19 became more fluorescent than did monocytes from HDs after being exposed to DCFH-DA ([Fig 1, B and C](#)). [Fig 1, C](#) shows the intensity of spontaneous monocytic ROS production in HDs, ICU patients, and non-ICU patients. The non-ICU patients produced more ROSs than the HDs did (22.2 ± 4.5 vs 17.2 ± 4.6 arbitrary units [AU] of mean fluorescence intensity [*t* test $P = .004$]), whereas the ICU patients did not (16.4 ± 3.9 vs 17.2 ± 4.6 AU [*t* test $P = .855$]). Yet, the ICU patients who survived had lower monocytic ROS production than those who did not (15.6 ± 3.4 vs 19.6 ± 4.1 AU [*t* test $P = .021$]) ([Fig 1, D](#)). To identify the monocyte subpopulations responsible for ROS production, we labeled the PBMCs exposed to DCFH-DA with anti-CD14 and anti-CD16 antibodies to identify classical ($CD14^{\text{high}}CD16^{\text{low}}$), intermediate ($CD14^+CD16^+$), and alternative ($CD14^{\text{low}}CD16^{\text{high}}$) monocytes ([Fig 1, E](#)). [Fig 1, F](#) shows that the intermediate and classical monocytes produced the highest amount of ROSs. Compared with the ICU participants, the non-ICU participants had a higher percentage of intermediate monocytes (median \pm interquartile range [IQR] = $20.7\% \pm 13.8\%$ vs $10.7\% \pm 16.2\%$ [Mann-Whitney $P = .055$]) ([Fig 1, G](#)). Logically, the proportions of intermediate monocytes and ROS-producing monocytes were correlated in patients with COVID-19 ($r = 0.373$; $P = .004$) ([Fig 1, H](#)).

Monocytes from patients with COVID-19 induce DNA damage via ROSs

ROSs can oxidize proteins, lipids, or DNA. We searched for the effect of monocytic ROS production on the DNA of bystander cells. For this purpose, we probed the presence of the phosphorylated form of the histone variant H2AX (γ -H2AX), which is a hallmark of chromosome breaks and DNA replication stress,¹⁴ in primary BJ fibroblasts cocultured with PBMCs from patients with COVID-19. In this assay, PBMCs were cocultured in transwells (ie, with no cell-to-cell contact with BJ cells). Camptothecin, a topoisomerase I inhibitor that induces replication-dependent DNA lesions, was used as a positive control, and PBMCs from HDs were included as negative controls. The PBMCs from 8 of the 25 patients tested (32%) induced γ -H2AX nuclear foci in bystander BJ cells, as exemplified in [Fig 2, A and B](#). [Fig 2, C](#) shows that the formation of these foci was prevented by preincubating PBMCs with the ROS scavenger NAC or the NADPH oxidase inhibitor DPI. This establishes that the γ -H2AX foci are indeed induced by ROSs. To be really sure that the sources of the DNA damaging ROSs were monocytes, we repeated the experiment after depleting a patient's PBMCs of monocytes by using CD14-coated magnetic beads. [Fig 2, D](#) shows that whereas the PBMCs and monocytes from the patient we analyzed induced DNA damage, monocyte-depleted PBMCs from the same patient did not.

PBMC DNA damage results in T-cell apoptosis during severe SARS-CoV-2 infection

ROS-induced DNA damage may provoke apoptosis.¹³ Therefore, we tested whether coculturing with COVID-19 PBMCs might trigger apoptosis in PBMCs from HDs. Indeed, at their surface, HD T cells had more phosphatidylserine (a marker of apoptosis), as measured by annexin V labeling on day 6, when they were exposed to COVID-19 PBMCs able to induce DNA damage than when they were exposed to another HD's PBMCs ($15.0\% \pm 1.5\%$ vs $10.8 \pm 1.7\%$ [*t* test $P = .034$]) ([Fig 2, E](#)). This programmed cell death provoked by COVID-19 PBMCs was entirely mediated by ROSs, because the presence of NAC reduced apoptosis to the background level observed in the

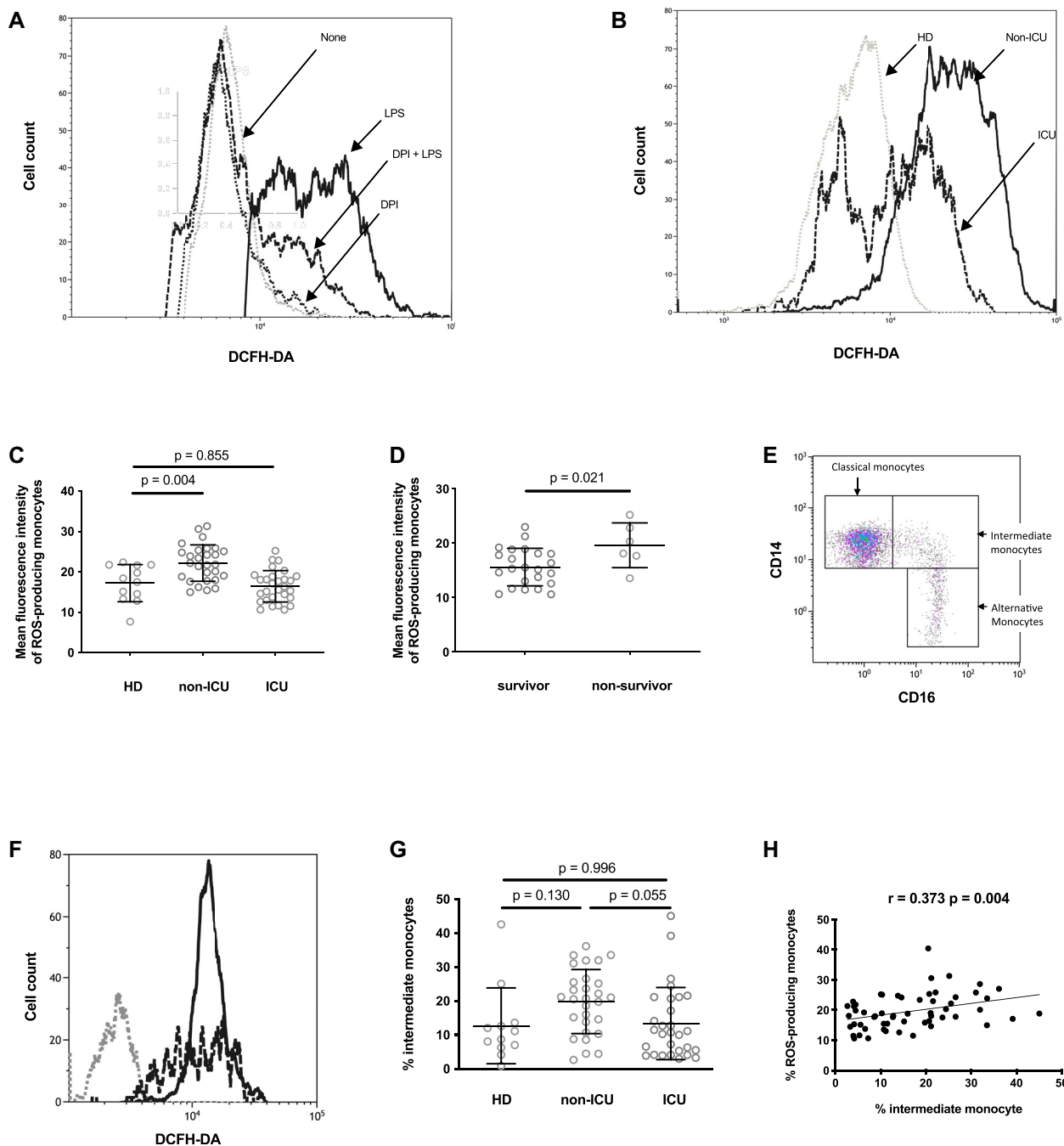


FIG 1. The monocytes from certain patients with COVID-19 spontaneously produce ROSs. **A**, Fluorescence in monocytes from an HD that have been preincubated (DPI + LPS [---] or not (LPS [---]) with the NADPH oxidase inhibitor DPI, exposed to DCFH-DA, and stimulated with LPS. As a negative control, we analyzed fluorescence in the same monocytes preincubated (DPI [---] or not (None [gray dots]) with DPI and exposed to DCFH-DA. **B**, Fluorescence in monocytes from an HD (---), a non-ICU patient (non-ICU [---]), and an ICU patient (ICU [---]) exposed to DCFH-DA. **C**, Mean fluorescence intensity of ROS-producing monocytes from HDs, non-ICU patients (non-ICU), and ICU patients (ICU) exposed to DCFH-DA. One-way ANOVA test ($P < .001$). **D**, Mean fluorescence intensity of ROS-producing monocytes from ICU patients who did or did not survive. **E**, Identification of the classical, intermediate, and alternative monocyte subpopulations by flow cytometry. **F**, Fluorescence in $CD14^{high}CD16^{low}$ (---), $CD14^{+}CD16^{+}$ (—), and $CD14^{low}CD16^{high}$ (---) monocytes from an ICU patient exposed to DCFH-DA. **G**, Percentages of $CD14^{-}CD16^{+}$ monocytes circulating in HDs, ICU patients, and non-ICU patients. One-way ANOVA test $P = .032$. **H**, Correlation between the proportions of intermediate and ROS-producing monocytes in ICU patients and non-ICU patients.

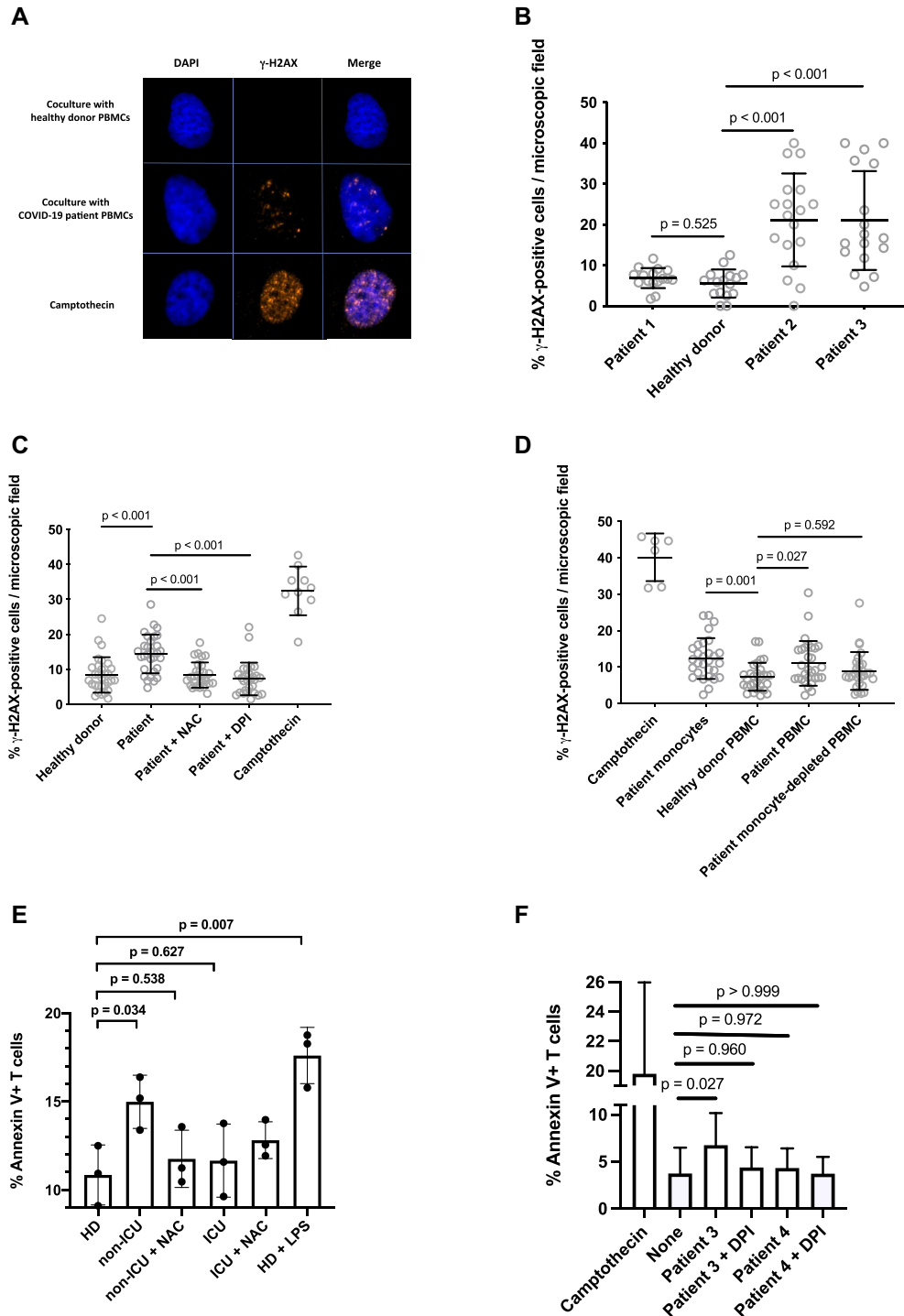


FIG 2. Monocytes from a patient with COVID-19 may induce DNA damage via ROSs. **A**, Detection of γ -H2AX foci by immunofluorescence in BJ cells cocultured with PBMCs from an HD or a patient with COVID-19. **B**, Quantification of the γ -H2AX foci induced in BJ fibroblasts by PBMCs from patients with COVID-19. Welch ANOVA test $P < .001$. **C**, γ -H2AX foci induced in BJ cells by PBMCs from a patient with COVID-19 are prevented by N-acetylcysteine or DPI. Kruskal-Wallis test $P < .001$. **D**, Monocytes isolated from a patient with COVID-19 induce DNA damage. The ability to induce γ -H2AX foci in the BJ fibroblasts of PBMCs from a patient with COVID-19, of the same PBMCs depleted of monocytes, and of monocytes isolated from these PBMCs was tested. Kruskal-Wallis test $P < .001$. **E**, Intensity of phosphatidylserine expression at the surface of HD PBMCs cocultured with PBMCs able to induce DNA damage treated (non-ICU + NAC) or not (non-ICU) with N-acetylcysteine, or with PBMCs unable to induce DNA damage treated (ICU + NAC) or not (ICU) with N-acetylcysteine. One-way ANOVA test $P = .002$. **F**, Intensity of phosphatidylserine expression at the surface of HD PBMCs cocultured with COVID-19 monocytes able (patient 3) or not able (patient 4) to induce DNA damage and treated with DPI (+DPI) or not treated.

presence of HD PBMCs ($11.8\% \pm 1.6\%$ vs $10.8\% \pm 1.7\%$ [t test $P = .939$]) (Fig 2, E). In contrast, coculturing with COVID-19 PBMCs unable to induce DNA damage or with HD PBMCs resulted in the same level of apoptosis ($11.7\% \pm 2.1\%$ vs $10.8\% \pm 1.7\%$ [t test $P = .959$]) (Fig 2, E). As a positive control, we used LPS-stimulated PBMCs, which triggered apoptosis in HD PBMCs ($17.6\% \pm 1.6\%$ vs $10.8\% \pm 1.7\%$ [t test $P = .001$]) (Fig 2, E). We obtained the same results when we cocultured purified COVID-19 monocytes able to cause DNA damage with HD PBMCs (Fig 2, F). The monocytes of a patient known to induce γ -H2AX foci in neighboring cells (patient 3) provoked apoptosis in cocultured PBMCs ($6.8\% \pm 3.4\%$ vs $3.7\% \pm 2.8\%$ [t test $P = .027$]) prevented by DPI ($4.4\% \pm 2.1\%$ vs $3.7\% \pm 2.8\%$ [t test $P = .980$]), whereas the monocytes of a patient (patient 4) unable to induce γ -H2AX foci in neighboring cells did not ($4.3\% \pm 2.1\%$ vs $3.7\% \pm 2.8\%$ [t test $P = .972$]).

PBMCs of patients with COVID-19 present with DNA damage

As the monocytes of certain patients with COVID-19 release ROSs that are able to cause DNA damage to neighboring cells, we analyzed whether the PBMCs of these patients presented with DNA damage. To do this, we looked for the presence of γ -H2AX nuclear foci in their PBMCs. Fig 3, A shows an example of a patient with COVID-19 whose PBMCs harbor such DNA damage markers. Globally, the proportion of DNA-damaged PBMCs was higher in the 19 non-ICU patients (median \pm IQR = $9.7\% \pm 4.0\%$ vs $5.8\% \pm 2.9\%$ [Mann-Whitney $P = .003$]), and the 28 ICU patients (median \pm IQR = $10.0\% \pm 8.4\%$ vs $5.8\% \pm 2.9\%$ [Mann-Whitney $P < .001$]) than in the age-matched HDs whose cells we analyzed (Fig 3, B). The PBMCs from a patient with COVID-19 also harbored DNA double-strand breaks, as revealed by the labeling with an antibody specific for 53BP1, which is a protein known to aggregate at double-strand ends.¹⁵ In the example shown in Fig 3, C, $16.8\% \pm 3.4\%$ of the patient PBMCs presented 53BP1 foci, which was a higher proportion than in the HD PBMCs ($6.9\% \pm 1.6\%$ [t test $P = .011$]). Next, we quantified CD4⁺ T-cell and CD8⁺ T-cell apoptosis in the participant peripheral blood. Fig 3, D shows that annexin V expression at the surface of both lymphocyte subpopulations, particularly on CD8⁺ T cells, was more frequent in the patients with COVID-19 than in the controls. We also tested whether the phenomenon that we have described could result in lymphopenia in patients with COVID-19. To this aim, we looked for a correlation between the intensity of DNA damage in PBMCs and lymphopenia. As shown in Fig 3, E, we observed an inverse correlation between the percentage of PBMCs with γ -H2AX foci and lymphocyte count in the patients and HDs analyzed ($r = -0.341$; $P = .025$).

AngII induces monocytic ROS production

SARS-CoV-2 downregulates the cell surface expression of angiotensin-converting enzyme 2 (ACE2), its main receptor, via ACE2 cointernalization and cleavage by the serine protease TMPRSS2.¹⁶ As ACE2 is known to convert AngII into angiotensin 1-7, this should result in an increase in AngII concentration.¹⁶ As AngII has been shown to induce ROS production in human mesangial cells,¹⁷ we tested whether this peptide is also able to provoke the release of ROSs by human monocytes. Indeed,

we observed that like LPS, AngII increased the fluorescence of HD monocytes preincubated with DCFH-DA (Fig 4, A). This effect was completely prevented by a 1-hour preincubation with DPI ($91.7\% \pm 15.3\%$ [Fig 4, B]) or the angiotensin receptor type 1 (AT1) antagonist losartan at $10 \mu\text{g}/\text{mL}$ ($98.7\% \pm 4.5\%$ [Fig 4, C]). Next, we checked to see whether the peripheral blood concentration of AngII was actually high in patients with COVID-19. Fig 4, D shows that plasma levels of AngII in non-ICU patients (median \pm IQR = 72.3 ± 68.6 vs 54.5 ± 73.3 pg/mL [Mann-Whitney test $P = .017$]) but not in ICU patients (median \pm IQR = 33.2 ± 31.5 vs 54.5 ± 73.3 pg/mL [Mann-Whitney test $P > .999$]) were higher than those in HDs. The lower level of AngII in ICU patients than in non-ICU patients might be the consequence of the increase in ACE2 expression reported in patients with severe COVID-19,¹⁸ driven by interferon¹⁹ and/or reoxygenation.²⁰ To test the hypothesis that AngII might be involved in the monocytic ROS overproduction that we revealed in certain patients, we looked for a link between AngII plasma levels and the intensity of ROS synthesis in HD, ICU, and non-ICU participants. Fig 4, E shows a clear correlation between these 2 parameters ($r = 0.299$; $P = .027$). This explains the fact that ROS expression was less intense in ICU patients than in non-ICU patients. Thereafter, we checked whether AngII-stimulated monocytes could induce DNA damage in BJ cells. Indeed, this was the case, and the DNA damage was prevented by DPI (Fig 4, F) and the AT1 antagonist losartan (Fig 4, G). We repeated the experiment with HD PBMCs instead of BJ cells (Fig 4, H). Again, we observed that AngII-activated monocytes were able to cause a DNA damage that was prevented by losartan or DPI. Furthermore, circulating levels of AngII were strongly correlated with the ability of patient PBMCs to induce DNA damage in BJ cells ($r = 0.704$; $P = .005$ [Fig 4, I]).

T-cell surface Fas expression is linked to ROS production

Our data are compatible with a model in which ROS-induced DNA damage provokes T-cell apoptosis. We have previously observed in severe COVID-19 that programmed T-cell death is also linked to T-cell surface expression of the death receptor Fas (CD95).²¹ ROSs are known to increase Fas expression in kidney cells,²² intestinal cells,²³ myogenic cells,²⁴ and neurons.²⁵ Conversely, in chronic granulomatous disease characterized by a defect in ROS production, patients express low T-cell surface levels of Fas.²⁶ Therefore, we searched for an association between monocytic ROS production and Fas expression on T cells in patients with COVID-19. Fig 4, J shows a strong link between these 2 parameters ($r = 0.461$; $P = .013$). Thus, ROSs released by monocytes could provoke apoptosis in T cells not only by breaking their DNA but also by inducing Fas expression at their surface.

DISCUSSION

In this study, we discovered a new pathogenic mechanism, namely, DNA damage and T-cell surface Fas overexpression due to AngII-driven ROS production by the monocytes of certain patients with COVID-19 and resulting in PBMC apoptosis (see Fig E1 in the Online Repository at www.jacionline.org). Of note, ICU patients exhibit more T-cell apoptosis and lymphopenia than non-ICU patients, whereas their plasma level of AngII and their monocytic ROS production are lower. The explanation for this

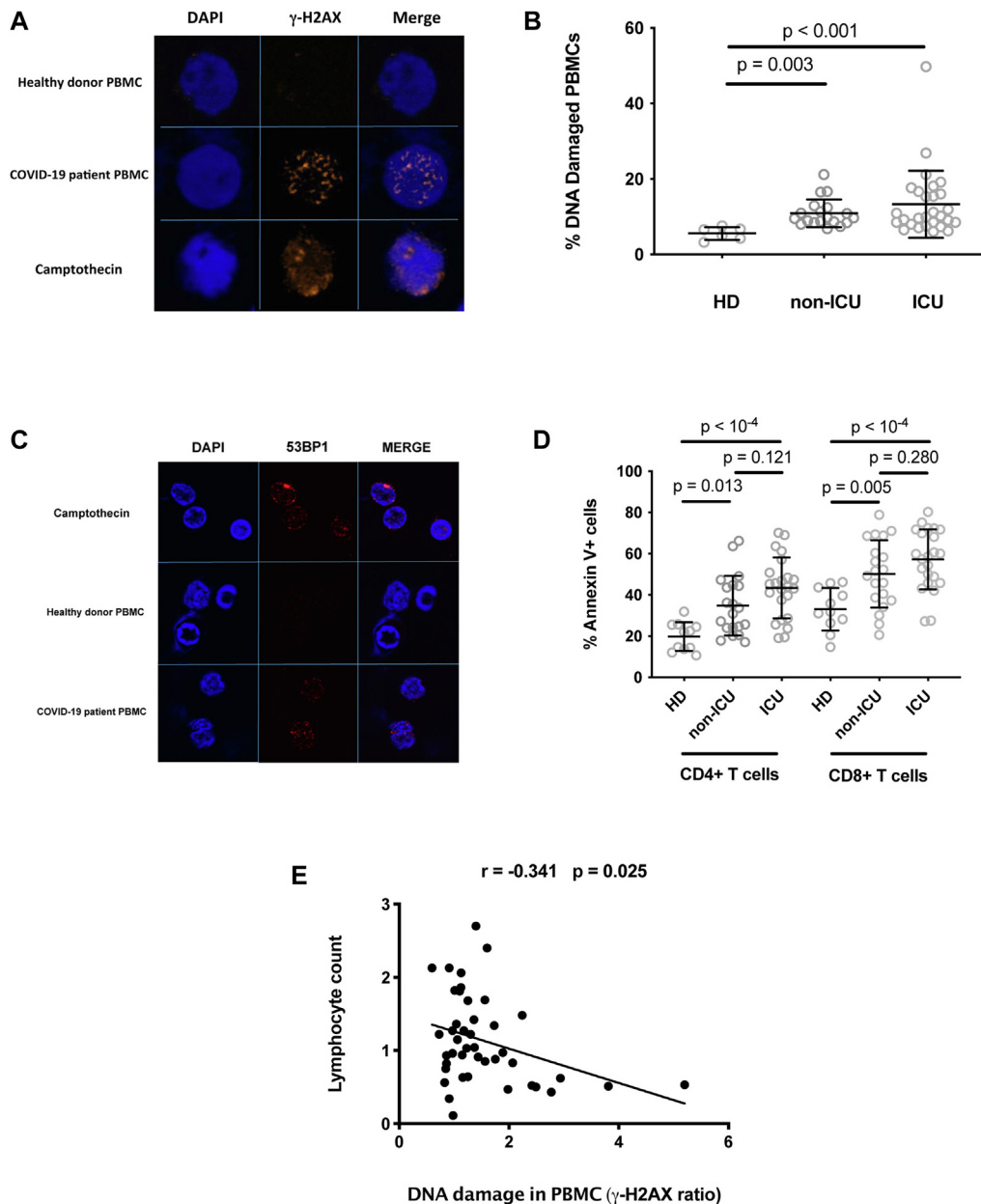


FIG 3. DNA damage in PBMCs from patients with COVID-19. **A**, PBMCs from a patient with COVID-19 whose monocytes induce DNA damage in bystander BJ cells spontaneously present with γ -H2AX foci. PBMCs from an HD treated with camptothecin or not treated were used as positive and negative controls, respectively. **B**, Percentages of PBMCs harboring γ -H2AX foci in HDs, non-ICU patients (non-ICU), and ICU patients (ICU). Kruskal-Wallis test $P = .002$. **C**, PBMCs from a patient with COVID-19 whose monocytes induce DNA damage in bystander BJ cells spontaneously present with 53BP1 foci. PBMCs from an HD treated with camptothecin or not treated were used as positive and negative controls, respectively. **D**, Annexin V expression on peripheral blood CD4⁺ T cells and CD8⁺ T cells of HDs, non-ICU patients (non-ICU), and ICU patients (ICU). One-way ANOVA test $P < .001$ for CD4⁺ T cells and $P < .001$ for CD8⁺ T cells. **E**, Correlation between the intensity of DNA damage in PBMC and lymphocyte counts. The intensity of DNA damage in PBMCs is expressed as the ratio of the percentage of patient PBMCs presenting γ -H2AX foci to the percentage of HD PBMCs presenting γ -H2AX foci.

apparent paradox might lie in the delay of a few days between DNA damage and apoptosis (for the speculative scenario, see Fig E2 in the Online Repository at www.jacionline.org). This delay could be due to the fact that cells first try to repair the damage, and thereafter, in the event of failure, trigger apoptosis.²⁷ Accordingly, we observed apoptosis in PBMCs cocultured with

patient monocytes only after 6 days (Fig 2, E and F). The non-ICU patients were at day 7 of the disease (Table I). SARS-CoV-2 had replicated, internalized ACE2, and thereby increased AngII plasma level (Fig 4, D). AngII had induced monocytic ROS production (Fig 1, B and C) responsible for DNA damage in T cells (Fig 3, B). At that time, T lymphocytes were possibly trying to

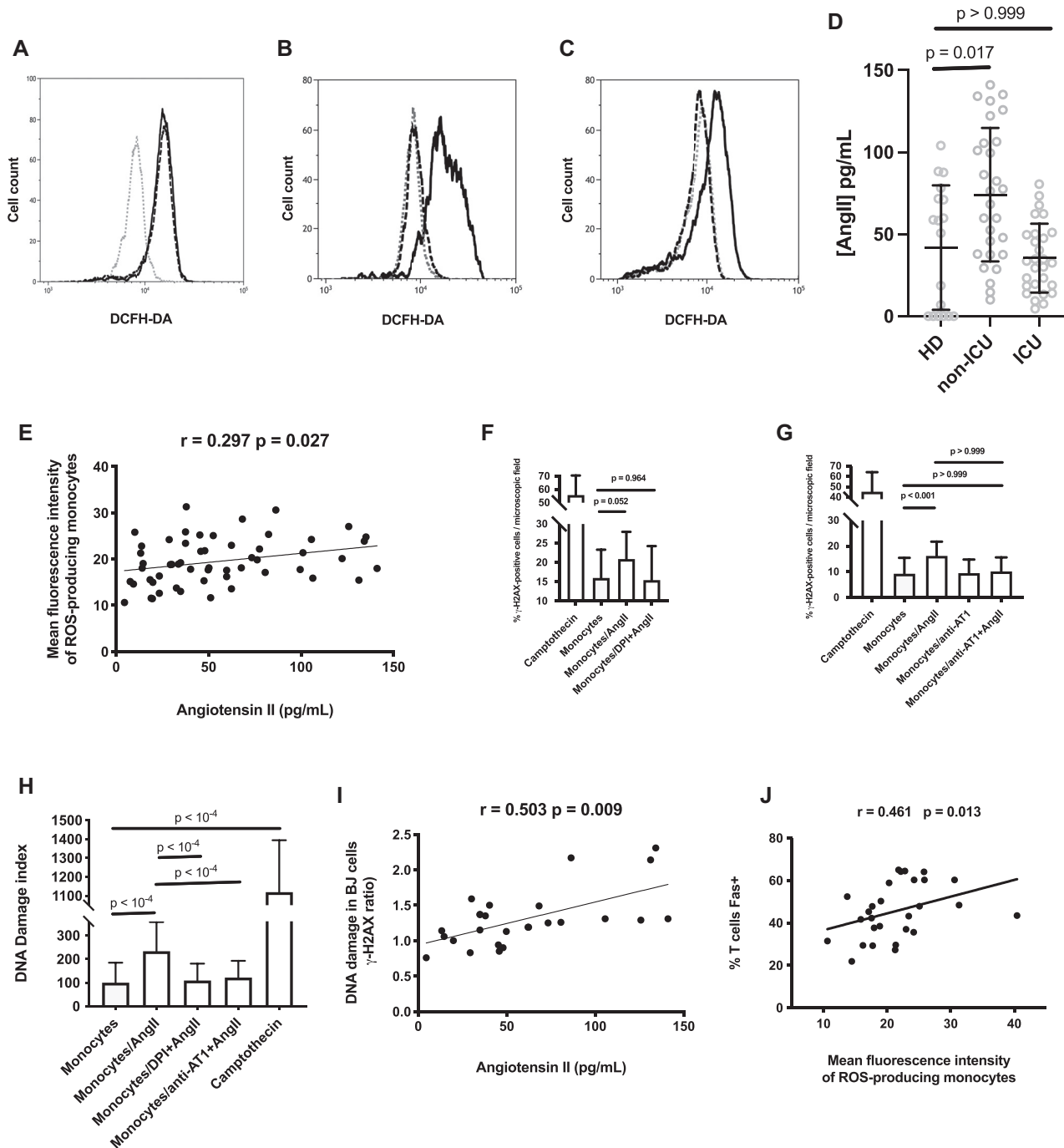


FIG 4. AngII induces ROS monocyctic production and DNA damage. Fluorescence in monocytes from an HD, preincubated or not (---) with LPS (---) or AngII (—) (**A**), AngII (—) or DPI and AngII (---) (**B**), AngII (—), or losartan and AngII (---), and exposed to DCFH-DA (**C**). **D**, Plasma levels of AngII in patients and controls. Kruskal-Wallis test $P = .001$. **E**, Correlation between plasma levels of AngII and monocyctic ROS production in patients and controls. **F-H**, AngII-activated monocytes induce DNA damage in neighboring cells. Ability of HD monocytes stimulated (monocytes/AngII) or not (monocytes) by AngII to cause γ -H2AX foci in bystander BJ cells (**F** and **G**) and HD PBMCs (**H**). The effect of the preincubation of monocytes with DPI (monocytes/DPI + AngII) (**F**) or AT1 antagonist (monocytes/anti-AT1 + AngII) (**G**) is shown. **F**, Welch ANOVA $P < .001$; **G** and **H**, Kruskal-Wallis test $P < .001$. **I**, Correlation between plasma levels of AngII and the ability of patient PBMCs to induce DNA damage, expressed as the ratio of the percentage of BJ cells presenting γ -H2AX foci in the presence of patient PBMCs to the percentage of BJ cells presenting γ -H2AX foci in the presence of HD PBMCs. **J**, Correlation between monocyctic ROS production and the percentage of T lymphocytes expressing Fas in patients.

repair this damage, a hypothesis accounting for the fact that the lymphopenia was not yet major. In this scenario, it was only a few days later that the consequence of this irreparable injury would have appeared clearly; lymphopenia occurred in ICU patients who were at day 12 of the disease (Table 1). In ICU patients, ROS expression was less intense than in non-ICU patients, probably owing to the lower AngII plasma level in the former than in the latter. This decrease in AngII concentration over time might be the consequence of the increase in ACE2 expression reported in severe COVID-19¹⁸ and driven by interferon¹⁹ and/or reoxygenation,²⁰ as well as by the decrease in viral load.²⁸ The amount of ROSs released by monocytes would then be insufficient to provoke T-cell apoptosis.

ROS-induced PBMC programmed cell death may have various deleterious effects. First, it may result in an immune deficiency favoring coinfections with other viruses,²⁹ bacteria,³⁰ or mycoses³¹ and in a poor immunologic memory, paving the way for SARS-CoV-2 reinfection. Second, regulatory T-cell apoptosis may account for the deficiency of regulatory T cells observed in severe forms of COVID-19,³² favoring immune activation. Third, CD8⁺ T-cell and NK cell loss due to programmed cell death might contribute to a cytokine storm. Indeed, these cytotoxic lymphocytes have been found to be involved in the downregulation of immune activation during the course of infections via their ability to kill T cells, NK cells, and antigen-presenting cells.^{33,34} Accordingly, in primary hemophagocytic lymphohistiocytosis, mutations resulting in cytolytic deficiency may provoke cytokine storms.³⁵ Thus, the programmed death of CD8⁺ T cells and NK cells could impair a negative feedback on immune activation. Fourth, CD4⁺ T lymphocyte apoptosis, particularly follicular helper T-cell apoptosis, which may account for the depletion of this subpopulation,³⁶ might explain the poor isotype switch and B memory observed in severe forms of COVID-19.³⁷

The release of ROSs could have direct effects in addition to these indirect effects. As ROSs are known to activate the proinflammatory transcription factor nuclear factor- κ B³⁸ and the NLRP3 inflammasome,³⁹ they could favor a cytokine storm in severe forms. Locally, the numerous monocytes and/or macrophages in the lower respiratory tract could also participate in endothelial cell and alveolar and vascular damage via ROSs.⁴⁰

As we found *in vitro* that ROSs released by COVID-19 monocytes induce DNA damage and apoptosis, as the proportion of DNA-damaged PBMCs that we measured in patients was correlated with their lymphopenia (a major prognostic marker in COVID-19), and as we found a link between the level of monocytic ROS expression in ICU patients and their survival, our data and the well-documented proinflammatory effect of ROSs argue for a role of this pathogenic pathway in the outcome of COVID-19. These findings could also explain why older people, males, patients with diabetes, and patients with prior cardiovascular diseases, who express low levels of ACE2,⁴¹ present with severe forms of COVID-19 more often.

The mechanism that we uncovered may also explain why SARS-CoV-2 variants with an enhanced affinity for their ACE2 receptor may be more pathogenic. Actually, these variants should provoke an increased ACE2 internalization, a higher level of AngII, greater monocytic ROS production, and thus more inflammation and more DNA damage, resulting in lymphopenia and immune deficiency.

From a therapeutic viewpoint, our data may explain the beneficial effects of AT1 antagonists⁴² and antioxidants⁴³ on

COVID-19 observed in certain clinical trials. Given all the potential consequences of ROS release in severe COVID-19, therapeutic strategies aimed at reducing AngII signaling via AT1, ROS production, and apoptosis deserve more consideration (see Fig E1).

We are grateful to the persons who volunteered for this study, to Teresa Sawyers for critical reading of the manuscript, to the biologic resource center of the Nîmes University Hospital, and to BioMedTech core facilities for their help with flow cytometry (INSERM US36, CNRS UMS2009, Paris, France).

Clinical implication: Unveiling this new pathogenic pathway opens up new therapeutic possibilities for COVID-19.

REFERENCES

- Zhou F, Yu T, Du R, Fan G, Liu Y, Liu Z, et al. Clinical course and risk factors for mortality of adult inpatients with COVID-19 in Wuhan, China: a retrospective cohort study. *Lancet* 2020;395:1054-62.
- Zhang X, Tan Y, Ling Y, Lu G, Liu F, Yi Z, et al. Viral and host factors related to the clinical outcome of COVID-19. *Nature* 2020;583:437-40.
- Fan BE, Chong VCL, Chan SSW, Lim GH, Lim KGE, Tan GB, et al. Hematologic parameters in patients with COVID-19 infection. *Am J Hematol* 2020;95:E131-4.
- Reshi ML. RNA viruses: ROS-mediated cell death. *Int J Cell Biol* 2014;2014:467452.
- Casola A, Burger N, Liu T, Jamaluddin M, Brasier AR, Garofalo RP. Oxidant tone regulates RANTES gene expression in airway epithelial cells infected with respiratory syncytial virus role in viral-induced interferon regulatory factor activation. *J Biol Chem* 2001;276:19715-22.
- Hosakote YM, Jantzi PD, Esham DL, Spratt H, Kurosky A, Casola A, et al. Viral-mediated inhibition of antioxidant enzymes contributes to the pathogenesis of severe respiratory syncytial virus bronchiolitis. *Am J Resp Crit Care Med* 2011;183:1550-60.
- Li Q, Wang L, Dong C, Che Y, Jiang L, Liu L, et al. The interaction of the SARS coronavirus non-structural protein 10 with the cellular oxido-reductase system causes an extensive cytopathic effect. *J Clin Virol* 2005;34:133-9.
- Vijay R, Hua X, Meyerholz DK, Miki Y, Yamamoto K, Gelb M, et al. Critical role of phospholipase A2 group IID in age-related susceptibility to severe acute respiratory syndrome-CoV infection. *J Exp Med* 2015;212:1851-68.
- Codo AC, Davanzo GG, Monteiro LB, de Souza GF, Muraro SP, Virgilio-da-Silva JV, et al. Elevated glucose levels favor SARS-CoV-2 infection and monocyte response through a HIF-1 α /glycolysis-dependent axis. *Cell Metab* 2020;32:437-46.e5.
- Violi F, Oliva A, Cangemi R, Ceccarelli G, Pignatelli P, Carnevale R, et al. Nox2 activation in Covid-19. *Redox Biol* 2020;36:101655.
- Moghaddam A, Heller RA, Sun Q, Seelig J, Cherkezov A, Seibert L, et al. Selenium deficiency is associated with mortality risk from COVID-19. *Nutrients* 2020;12:2098.
- Thomas T, Stefanoni D, Reisz JA, Nemkov T, Bertolone L, Francis RO, et al. COVID-19 infection alters kynurenine and fatty acid metabolism, correlating with IL-6 levels and renal status. *JCI Insight* 2020;5:e140327.
- Darzynkiewicz Z, Zhao H, Halicka HD, Rybak P, Dobrucki J, Wlodkowic D. DNA damage signaling assessed in individual cells in relation to the cell cycle phase and induction of apoptosis. *Crit Rev Clin Lab Sci* 2012;49:199-217.
- Valdiglesias V, Giunta S, Fenech M, Neri M, Bonassi S. GammaH2AX as a marker of DNA double strand breaks and genomic instability in human population studies. *Mutation Res* 2013;753:24-40.
- Panier S, Boulton SJ. Double-strand break repair: 53BP1 comes into focus. *Nat Rev Mol Cell Biol* 2014;15:7-18.
- Xavier LL, Ribas Neves PF, Paz LV, Neves LT, Bagatini PB, Saraiva Macedo Timmers LF, et al. Does angiotensin II peak in response to SARS-CoV-2? *Front Immunol* 2021;11:577875.
- Chen Y, Zhang A-H, Huang S-M, Ding G-X, Zhang W-Z, Bao H-V, et al. NADPH oxidase-derived reactive oxygen species involved in angiotensin II-induced monocyte chemoattractant protein-1 expression in mesangial cells. *Zhonghua Bing Li Xue Za Zhi* 2009;38:456-61.
- Amati F, Vancheri C, Latini A, Colona VL, Grelli S, D'Apice MR, et al. Expression profiles of the SARS-CoV-2 host invasion genes in nasopharyngeal and oropharyngeal swabs of COVID-19 patients. *Heliyon* 2020;6:e05143.
- Ziegler CGK, Allon SJ, Nyquist S, Mbano IM, Miao VN, Tzouanas CN, et al. SARS-CoV-2 receptor ACE2 is an interferon-stimulated gene in human airway

- epithelial cells and is detected in specific cell subsets across tissues. *Cell* 2020;181:1016-35.
20. Wing PAC, Keeley TP, Zhuang X, Lee JY, Prange-Barczynska M, Tsukuda S, et al. Hypoxic and pharmacological activation of HIF inhibits SARS-CoV-2 infection of lung epithelial cells. *Cell. Rep* 2021;35:109020.
 21. Andre S, Picard M, Cezar R, Roux-Dalvai F, Alleaume-Butaux A, Soundaramourty C, et al. T cell apoptosis characterizes severe Covid-19 disease. *Cell Death Differ* 2022;1-14. <https://doi.org/10.1038/s41418-022-00936-x>.
 22. Tsuruya K, Tokumoto M, Ninomiya T, Hirakawa M, Masutani K, Taniguchi M, et al. Antioxidant ameliorates cisplatin-induced renal tubular cell death through inhibition of death receptor-mediated pathways. *Am J Physiol Renal Physiol* 2003;285:F208-18.
 23. Denning TL, Takaishi H, Crowe SE, Boldogh I, Jevnikar A, Ernst PB. Oxidative stress induces the expression of Fas and Fas ligand and apoptosis in murine intestinal epithelial cells. *Free Radic Biol Med* 2002;33:1641-50.
 24. Wang G, Jiang L, Song J, Zhou SF, Zhang H, Wang K, et al. Mip1 protects H9c2 myogenic cells from hydrogen peroxide-induced apoptosis through inhibition of the expression of the death receptor Fas. *Int J Mol Sci* 2014;15:18206-20.
 25. Facchinetti F, Furegato S, Terrazzino S, Leon A. H(2)O(2) induces upregulation of Fas and Fas ligand expression in NGF-differentiated PC12 cells: modulation by cAMP. *J Neurosci Res* 2002;69:178-88.
 26. Montes-Berrueta D, Ramirez L, Salmen S, Berrueta L. Fas and FasL expression in leukocytes from chronic granulomatous disease patients. *Invest Clin* 2012;53:157-67.
 27. De Zio D, Cianfanelli V, Vecconi F. New insights into the link between DNA damage and apoptosis. *Antioxid Redox Signal* 2013;19:559-71.
 28. Boef AGC, van Wezel EM, Gard L, Netkova K, Lokate M, van der Voort PHJ, et al. Viral load dynamics in intubated patients with COVID-19 admitted to the intensive care unit. *J Crit Care* 2021;64:219-25.
 29. Abouelkhair MA. Non-SARS-CoV-2 genome sequences identified in clinical samples from COVID-19 infected patients: Evidence for co-infections. *PeerJ* 2020;8:e10246.
 30. Rodriguez-Nava G, Yanez-Bello MA, Trelles-Garcia DP, Chul Won Chung CW, Goar Egoryan G, Harvey J, et al. A retrospective study of coinfection of SARS-CoV-2 and *Streptococcus pneumoniae* in 11 hospitalized patients with severe COVID-19 pneumonia at a single center. *Med Sci Monit* 2020;26:e928754.
 31. Segrelles-Calvo G, de S Araújo GR, Frases S. Systemic mycoses: a potential alert for complications in COVID-19 patients. *Future Microbiol* 2020;15:1405-13.
 32. Meckiff BJ, Ramirez-Suástegui C, Fajardo V, Chee SJ, Kusnadi A, Simon H, et al. Imbalance of regulatory and cytotoxic SARS-CoV-2-reactive CD4 + T cells in COVID-19. *Cell* 2020;183:1-14.
 33. Crouse J, Bedenikovic G, Wiesel M, Ibberson M, Xenarios I, Von Laer D, et al. Type I interferons protect T cells against NK cell attack mediated by the activating receptor NCR1. *Immunity* 2014;40:961-73.
 34. Madera S, Rapp M, Firth MA, Beilke JN, Lanier LL, Sun JC. Type I IFN promotes NK cell expansion during viral infection by protecting NK cells against fratricide. *J Exp Med* 2016;213:225-33.
 35. Soy M, Atagündüz P, Atagündüz I, Sucak GT. Hemophagocytic lymphohistiocytosis: a review inspired by the COVID-19 pandemic. *Rheumatol Int* 2021;41:7-18.
 36. Duan Y-Q, Xia M-H, Ren L, Zhang Y-F, Ao Q-L, Xu S-P, et al. Deficiency of Tfh cells and germinal center in deceased COVID-19 patients. *Curr Med Sci* 2020;40:618-24.
 37. Newell KL, Clemmer DC, Cox JB, Kayode YI, Zoccoli-Rodriguez V, Taylor HE, et al. Switched and unswitched memory B cells detected during SARS-CoV-2 convalescence correlate with limited symptom duration. *medRxiv* 2020:2020.09.04.20187724.
 38. Morgan MJ, Liu Z-G. Crosstalk of reactive oxygen species and NF-κB signaling. *Cell Res* 2011;21:103-15.
 39. Harijith A, Ebenezer DL, Natarajan V. Reactive oxygen species at the crossroads of inflammasome and inflammation. *Front Physiol* 2014;5:352.
 40. Rendeiro AF, Ravichandran H, Bram Y, Salvatore S, Borczuk A, Elemento O, et al. The spatio-temporal landscape of lung pathology in SARS-CoV-2 infection. *medRxiv* 2020:2020.10.26.20219584.
 41. Verdecchia P, Cavallini C, Spanevello A, Angeli F. The pivotal link between ACE2 deficiency and SARS-CoV-2 infection. *Eur J Intern Med* 2020;76:14-20.
 42. Saavedra JM. Angiotensin receptor blockers are not just for hypertension anymore. *Physiology (Bethesda)* 2021;36:160-73.
 43. Mohanty RR, Padhy BM, Das S, Meher BR. Therapeutic potential of N-acetyl cysteine (NAC) in preventing cytokine storm in COVID-19: review of current evidence. *Eur Rev Med Pharmacol Sci* 2021;25:2802-7.

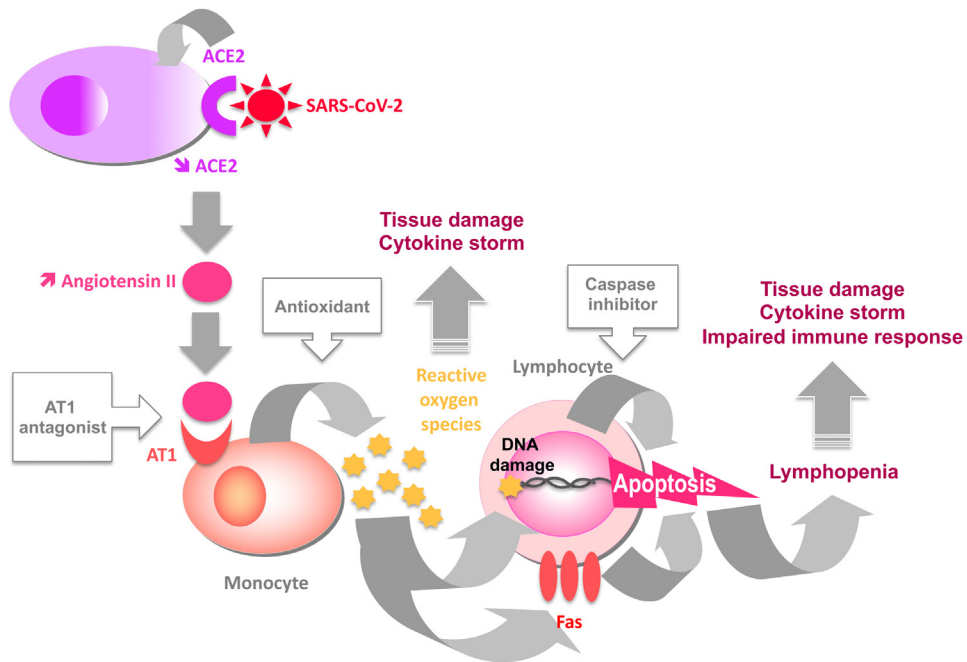


FIG E1. Cascade of events leading to lymphopenia in severe forms of COVID-19. Boxed molecules are blocking the step indicated in the figure.

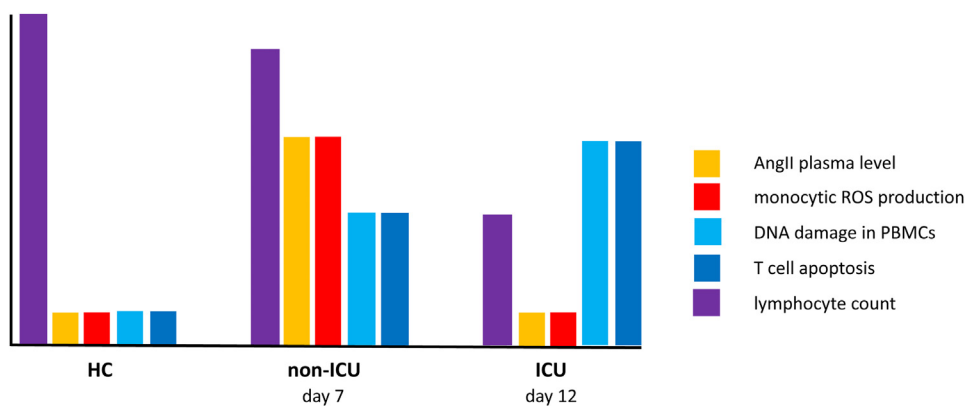


FIG E2. Kinetics of the events leading to lymphopenia in severe forms of COVID-19. Non-ICU patients are at day 7: their AngII plasma level and monocyte ROS production are strongly increased, DNA damage in their PBMCs and their T-cell apoptosis are moderately elevated, and their lymphocyte count is slightly decreased. ICU patients are at day 12: their AngII plasma level and monocyte ROS production are normal, DNA damage in their PBMCs and their T-cell apoptosis are strongly elevated, and their lymphocyte count is drastically decreased.